Title: A derivation error exists in the current implementation of the Johnson et al. (1942) modified Arrhenius function that affects leaf carbon balance models

Running Title: Derivation error in modified Arrhenius model

Author: Bridget Murphy[1], Joseph R. Stinziano[2,*]

Affiliations: [1] Department of Biology, University of Western Ontario, London, ON, Canada;

[2] Department of Biology, University of New Mexico, Albuquerque, NM, USA

[*] Corresponding author; Email: jstinziano@unm.edu; Tel: +1 (226) 678-1670

Article Type: Research Article

Word Count: 3,040

Introduction: 490

Material & Methods: 813

Results: 1154

Discussion: 557

Acknowledgments: 26

Number of Tables: 2

Number of Figures: 6

Abstract

Understanding biological temperature responses is crucial to predicting global carbon fluxes. The current approach to modeling photosynthetic temperature responses in large scale modeling efforts uses a modified Arrhenius equation. We rederived the modified Arrhenius equation from the source publication and uncovered a missing term that was dropped between 1942 and 2002. We compare fitted temperature response parameters between the new and old derivation of the modified Arrhenius equation. We find that most parameters are minimally affected, though small errors still exist. We then scaled the impact of these small errors to whole plant carbon balance and found that the impact of the rederivation of the Arrhenius on modelled daily carbon gain causes a meaningful deviation of ~1.8%. This suggests that the error in the derivation of the modified Arrhenius equation has impacted predictions of carbon fluxes at larger scales. We argue that it is time to move beyond the modified Arrhenius paradigm since the current implementation is categorically incorrect and to use more thermodynamically-grounded temperature response equations going forward.

Keywords: Arrhenius, temperature, photosynthesis, gas exchange, modeling, carbon balance

Introduction

Globally, photosynthesis and autotrophic respiration are the largest biological carbon fluxes, with photosynthesis removing ~120 Gt C year^{-1} and autotrophic respiration releasing ~60 Gt C year^{-1} (Amthor, 2000; Ciais et al., 2013). Given the temperature sensitivity of these large carbon fluxes, understanding how photosynthesis and respiration respond on acute, acclimatory, and adaptive timescales is crucial for predicting vegetative and carbon cycle responses to future global climates (Rogers et al., 2017; Stinziano et al. 2018). Biological temperature responses including photosynthesis and respiration are typically assumed to be exponential or peaked (Way and Yamori, 2014; Smith & Dukes, 2017; Kumarathunge et al., 2019). Exponential responses are usually modelled based on an Arrhenius-type curve (Arrhenius, 1915):

$$f(T) = Ae^{\frac{-E_a}{RT}} \qquad \text{Equation 1}$$

$$f(T) = k_{25}e^{\left[\frac{E_a(T-298.15)}{RT298.15}\right]} \qquad \text{Equation 2}$$

where f(T) is the rate of the process at temperature, A is a pre-exponential factor, T in K, k_{25} is the rate of the process at 298.15 K, E_a is the activation energy in J mol^{-1}, R is the universal gas constant of 8.314 J mol^{-1} K^{-1}, and 298.15 is the reference temperature in K. As for peaked responses, while a few options are available (Kruse et al., 2008; Hobbs et al., 2013; Heskel et al., 2016), the most commonly implemented version is the modified Arrhenius model of Johnson et al. (1942) as presented in Medlyn et al. (2002):

$$f(T) = k_{25}e^{\left[\frac{E_a(T-298.15)}{RT298.15}\right]}\left[\frac{1+e^{\frac{298.15\Delta S-H_d}{298.15R}}}{1+e^{\frac{T\Delta S-H_d}{TR}}}\right] \qquad \text{Equation 3}$$

where H_d is the deactivation energy in J mol^{-1}, and ΔS is the entropy of the process in J mol^{-1}.

Equation 3 is used for modeling the temperature responses of photosynthetic capacity (based on Farquhar et al., 1980): maximum carboxylation capacity of rubisco, V_{cmax}, maximum electron transport capacity, J_{max}, and related kinetics as well as Sharkey (1985) and Harley & Sharkey (1991) in their

calculation of triose phosphate utilization capacity (TPU). These parameters are then used in ecophysiological studies to understand thermal acclimation of photosynthesis (see Kattge & Knorr, 2007; Smith & Dukes, 2017; and Kumarathunge et al., 2019 for examples). Furthermore, this equation is also used in terrestrial biosphere models to predict the future state of the Earth system (e.g. Rogers et al., 2017).

Due to its ubiquity, we revisited the original Johnson et al. (1942) modified Arrhenius function to rederive Equation 3. In the process of this rederivation, we uncovered a term that was dropped sometime between Johnson et al. (1942) and Medlyn et al. (2002) which causes a systematic error in the application of Equation 3 in calculations covering individual species (e.g. Medlyn et al., 2002) to global scale processes (e.g. Rogers et al., 2017). We then refit a freely available dataset (Kumarathunge et al., 2019), with both versions of the modified Arrhenius model, and fed the temperature response fits through a carbon balance model to estimate the impact of the derivation error on modelled plant carbon balance. We predicted that the derivation error would cause substantial variation in fitted temperature response parameters, and that these differences would propagate through to modelled daily carbon balance.

Materials & methods

Rederivation of the modified Arrhenius equation

Johnson et al. (1942, equation 24) describe the temperature response of the light intensity of a luciferase reaction as:

$$I = \frac{c'' T e^{\frac{-\Delta H\ddagger}{RT}}}{1+e^{\frac{\Delta S}{R}} e^{\frac{-\Delta H}{RT}}} \qquad \text{Equation 4}$$

where I is the intensity of the luciferase reaction, c'' is not explicitly defined in Johnson et al. (1942), but presumably represents a second derivative of the rate, T is the temperature in K, R is the universal gas constant of 8.314 J mol^{-1} K^{-1}, ΔH‡ is the activation energy in J mol^{-1}, ΔH is the deactivation energy in J mol^{-1}, and ΔS is the entropy in J mol^{-1}. We can relativize the equation to a reference temperature:

$$\frac{I}{I_{25}} = \frac{\frac{c''Te^{\frac{-\Delta H\ddagger}{RT}}}{1+e^{\frac{\Delta S}{R}}e^{\frac{-\Delta H}{RT}}}}{\frac{c''298.15e^{\frac{-\Delta H\ddagger}{R298.15}}}{1+e^{\frac{\Delta S}{R}}e^{\frac{-\Delta H}{R298.15}}}} \qquad \text{Equation 5}$$

$$\frac{I}{I_{25}} = \frac{c''Te^{\frac{-\Delta H\ddagger}{RT}}}{c''298.15e^{\frac{-\Delta H\ddagger}{R298.15}}} \frac{1+e^{\frac{\Delta S}{R}}e^{\frac{-\Delta H}{R298.15}}}{1+e^{\frac{\Delta S}{R}}e^{\frac{-\Delta H}{RT}}} \qquad \text{Equation 6}$$

$$\frac{I}{I_{25}} = \frac{T}{298.15}e^{\frac{-\Delta H\ddagger}{RT}-\frac{-\Delta H\ddagger}{R298.15}} \frac{1+e^{\frac{\Delta S}{R}+\frac{-\Delta H}{R298.15}}}{1+e^{\frac{\Delta S}{R}+\frac{-\Delta H}{RT}}} \qquad \text{Equation 7}$$

$$I = I_{25}\frac{T}{298.15}e^{\left[\frac{-\Delta H\ddagger 298.15 - -\Delta H\ddagger T}{RT298.15}\right]}\left[\frac{1+e^{\frac{298.15\Delta S+-\Delta H}{298.15R}}}{1+e^{\frac{T\Delta S+-\Delta H}{TR}}}\right] \qquad \text{Equation 8}$$

$$I = I_{25}\frac{T}{298.15}e^{\left[\frac{\Delta H\ddagger(T-298.15)}{RT298.15}\right]}\left[\frac{1+e^{\frac{298.15\Delta S-\Delta H}{298.15R}}}{1+e^{\frac{T\Delta S-\Delta H}{TR}}}\right] \qquad \text{Equation 9}$$

Harmonizing the notation scheme to that typically used in plant ecophysiology:

$$f(T) = k_{25}\frac{T}{298.15}e^{\left[\frac{E_a(T-298.15)}{RT298.15}\right]}\left[\frac{1+e^{\frac{298.15\Delta S-H_d}{298.15R}}}{1+e^{\frac{T\Delta S-H_d}{TR}}}\right] \qquad \text{Equation 10}$$

Note the difference between Equations 3 and 10: the term T / 298.15 is missing from Equation 3. This introduces multiple systematic errors:

1) fitted parameters E_a, H_d, and ΔS;
2) scaling the rate variable using the wrong equation;
3) acclimation of E_a, H_d, and/or ΔS as errors due to 1) at each acclimation temperature.

Here we focus on the impact of 1 and 2 on modeling whole-plant carbon balance.

Data analysis

Using data from Kumarathunge et al. (2019), available from Kumarathunge et al. (2018), we fit Equations 3 and 10 to the data, both setting H_d to 200 kJ mol^{-1} and allowing H_d to be fit. We used the

R package {minpack.lm} (Elzhov et al., 2016) with starting parameters of E_a = 40 kJ mol^{-1}, ΔS = 0.650 kJ mol^{-1}, k_{25} = mean(parameter), and H_d (when fitted) varying from 1 to 500 kJ mol^{-1}, followed by the {BIC} function to select the best model based on Bayesian Information Criteria. We obtained 92 successful curve fits for the fixed H_d case, and 84 successful curve fits for the fitted H_d case. This allows us to explore the impact of the missing term on the output data under a typical fitting scenario (H_d is fixed) and under the full fitting scenario.

Modeling

We modelled the impact of the equations 3 and 10 on daily net plant carbon balance under conditions of H_d = 200 kJ mol^{-1} and fitted H_d. Data for leaf area, root and shoot masses, as well as leaf dark respiration at 25 °C were taken for white spruce (*Picea glauca*) from Stinziano & Way (2017), while stomatal conductance model parameters were calculated with the gas exchange data reported in Stinziano & Way (2017). Mean data were taken from the control treatment at weeks 0 and 12 to provide contrasting biomass allocation patterns such that week 0 is a low respiration scenario and week 12 is a high respiration scenario. These different respiration scenarios were used to reduce bias in any conclusions regarding the impact of Equations 3 and 10 on carbon balance, as the ratio of photosynthesis to respiration may alter the sensitivity of carbon balance to the Arrhenius equation used. Root respiration for white spruce was taken from Weger and Guy (1991) and we assumed that stem respiration was equal to root respiration (Table 1).

Table 1. Parameters used in modeling daily carbon gain.

Parameter	Group	Value	Reference
Respiration	R_{dark}	2.78 µmol m^{-2} s^{-1}	Stinziano & Way, 2017
	R_{day}	0.7 * R_{dark}	Ayub et al., 2011
	R_{root}	0.0095 µmol g^{-1} s^{-1}	Weger & Guy, 1991
	R_{stem}	0.0095 µmol g^{-1} s^{-1}	Assumed
	Q_{10}	2.015	Atkin & Tjoelker, 2003
Γ*	25 °C	42.75 µmol mol^{-1}	Bernacchi et al., 2001
	E_a	37.83 kJ mol^{-1}	Bernacchi et al., 2001
K_m	25 °C	718.4 µmol mol^{-1}	Bernacchi et al., 2001
	E_a	65.51 kJ mol^{-1}	Bernacchi et al., 2001
α		0.8	Norman & Campbell, 1998
ϕ		0.08	Norman & Campbell, 1998
Leaf Area	Low R	0.015 m^2	Stinziano & Way, 2017
	High R	0.025 m^2	Stinziano & Way, 2017

Stem Mass	Low R	0.496 g	Stinziano & Way, 2017
	High R	2.523 g	Stinziano & Way, 2017
Root Mass	Low R	0.498 g	Stinziano & Way, 2017
	High R	5.072 g	Stinziano & Way, 2017

Q_{10}: thermal sensitivity coefficient; Γ*: photorespiratory CO_2 compensation point; K_m: Michaelis-Menten constant for rubisco; α: absorbance of photosynthetically activation radiation; ϕ: maximum quantum efficiency of photosynthetic electron transport; E_a: activation energy; R_{dark}: leaf respiration in the dark; R_{day}: leaf respiration in the light; R_{root}: root respiration; R_{stem}: stem respiration; Low R: low respiration scenario; High R: high respiration scenario.

For the full model structure and equations, please see the accompanying R package {arrhenius.comparison} ("arrhenius.comparison_1.0.0.tar.gz"; Stinziano & Murphy, 2020) (see Table 2 for equations). Briefly, we linked the Medlyn et al. (2011) stomatal conductance model with the Farquhar et al. (1980) C_3 photosynthesis model, assuming infinite mesophyll conductance to CO_2 as these assumptions were used in fitting the data from Kumarathunge et al. (2018). Photosynthetic capacity, both maximum rubisco carboxylation capacity, V_{cmax}, and maximum electron transport rate, J_{max} were scaled to temperature using either Equation 3 or 10, while respiration was scaled according to (Atkin & Tjoelker, 2003). Photosynthesis and respiration were summed across each modelled day to calculate daily plant carbon assimilation.

Table 2. Equations used in modeling daily carbon uptake.

Equation	Reference
$f(T) = k_{25} Q_{10}^{\frac{T-298.15}{10}}$	Atkin & Tjoelker, 2003
$f(T) = k_{25} e^{\left[\frac{E_a(T-298.15)}{RT298.15}\right]}$	Arrhenius, 1915
$f(T) = k_{25} e^{\left[\frac{E_a(T-298.15)}{RT298.15}\right]} \left[\frac{1+e^{\frac{298.15\Delta S-H_d}{298.15R}}}{1+e^{\frac{T\Delta S-H_d}{TR}}}\right]$	Johnson et al., 1942; Medlyn et al., 2002
$f(T) = k_{25} \frac{T}{298.15} e^{\left[\frac{E_a(T-298.15)}{RT298.15}\right]} \left[\frac{1+e^{\frac{298.15\Delta S-H_d}{298.15R}}}{1+e^{\frac{T\Delta S-H_d}{TR}}}\right]$	Johnson et al., 1942; this study
$W_c = V_{cmax} \frac{C_i - \Gamma *}{C_i + K_m}$	Farquhar et al., 1980

$$W_j = min\left(J_{max}, \alpha\phi Q_{in}\frac{C_i - \Gamma *}{C_i + 2\Gamma *}\right)$$	Farquhar et al., 1980; Way et al., 2011
$$A_{gross} = min(W_c, W_j)$$	
$$A_{net} = A_{gross} - R_{day}$$	
$$g_s = g_0 + 1.6\left(1 + \frac{g_1}{\sqrt{VPD}}\right)\left(\frac{A_{net}}{C_a}\right)$$	Medlyn et al., 2011
$$C_i = C_a - 1.6\frac{A_{net}}{g_s}$$	
$$A_{plant} = A_{net} \times LA - R_{dark} \times LA - R_{stem} \times SM - R_{root} \times RM$$	
$$C_{balance} = \sum A_{plant} \times 3600 \times \frac{12.01}{1{,}000{,}000}$$	

f(T): rate of a process at a given temperature; T: temperature in K; k_{25}: rate of a process at 25 °C; Q_{10}: thermal sensitivity coefficient; E_a: activation energy in kJ mol^{-1}; ΔS: entropy parameter in kJ mol^{-1}; H_d: deactivation energy in kJ mol^{-1}; R: universal gas constant in 0.008314 kJ mol^{-1} K^{-1}; W_c: rate of CO_2-limited carboxylation in µmol m^{-2} s^{-1}; W_j: rate of RuBP regeneration-limited carboxylation in µmol m^{-2} s^{-1}; V_{cmax}: maximum rate of rubisco carboxylation capacity in µmol m^{-2} s^{-1}; J_{max}: maximum rate of electron transport in µmol m^{-2} s^{-1}; C_i: intercellular CO_2 concentration in µmol mol^{-1}; Γ*: photorespiratory CO_2 compensation point in µmol mol^{-1}; K_m: Michaelis-Menten constant for rubisco in µmol mol^{-1}; α: absorbance of photosynthetically active radiation; ϕ: maximum quantum efficiency of electron transport; Q_{in}: incident photosynthetically active radiation; A_{gross}: gross CO_2 assimilation in µmol m^{-2} s^{-1}; A_{net}: net CO_2 assimilation in µmol m^{-2} s^{-1}; R_{day}: leaf day respiration in µmol m^{-2} s^{-1}; g_s: stomatal conductance to water in mol m^{-2} s^{-1}; g_o: intercept for the Medlyn et al. 2011 model; g_1: slope for the Medlyn et al. 2011 model; VPD: vapor pressure deficit in kPa; C_a: CO_2 concentration at the leaf surface in µmol mol^{-1}; A_{plant}: whole plant net CO_2 assimilation; LA: leaf area in m^{-2}; R_{dark}: leaf dark respiration in µmol m^{-2} s^{-1}; R_{stem}: stem respiration in µmol m^{-2} s^{-1}; R_{root}; root respiration in µmol m^{-2} s^{-1}; SM: stem mass in g; RM: root mass in g; $C_{balance}$: whole plant daily carbon balance in g plant^{-1} day^{-1}.

Modeling was performed on 18 total days of environmental data, with three days of data from three months (17th – 19th of May, August, and October, 2019) obtained from external irradiance sensors at the Biotron Experimental Climate Change Research Centre at the University of Western Ontario and

the remaining environmental data from Environment Canada historical climate data for South London (43.01°N, 81.27°W, altitude: 251 m) and the rooftop greenhouse at the University of New Mexico (35.08°N, 106.62°W, altitude: 1587 m) to capture different levels of environmental variability (Fig. 1).

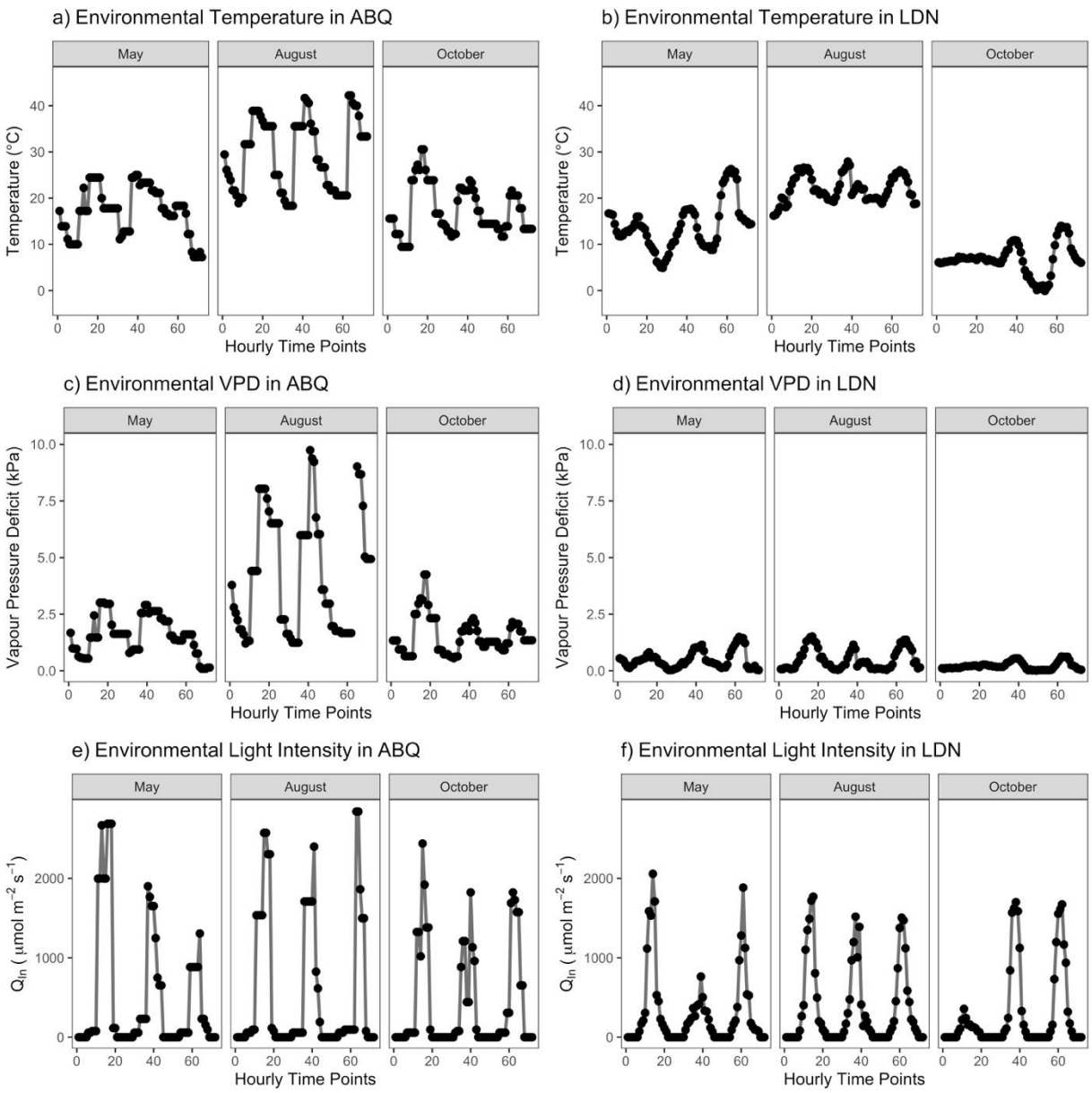

Figure 1. Environmental data used to drive the model in Table 1 covering 3 days (17th, 18th, and 19th) of 3 months. (a,c,e) Albuquerque, NM, USA; (b,d,e) London, ON, Canada.

Overall, the modeling approach allows us to assess the relative differences between Equations 3 and 10 under a low- and high- respiration scenario, fixing versus fitting H_d, and across different ranges of seasonal variability.

Statistical analysis

Data were analyzed using the {lm} function in R v.3.6.1 (R Core Team, 2019), regressing the data obtained from Equation 10 against the data obtained from Equation 3. All code and data will be made freely available on GitHub upon publication in the {arrhenius.comparison} R package (Stinziano & Murphy, 2020).

Results

Fixed H_d of 200 kJ mol^{-1}

Incorporating the missing term into Equation 3 to produce Equation 10 caused small differences in the fitting of E_a for V_{cmax}, with a slope of 0.997 ± 0.001 and intercept of -2.162 ± 1.19 · 10^{-1} kJ mol^{-1} ($F_{1,90}$ = 4.56 · 10^5, R^2 = 0.9998, P < 2.2 · 10^{-16}) (Fig. 2b). For ΔS, the slope was 0.991 ± 3 · 10^{-3} and an intercept of 0.005 ± 2 · 10^{-3} kJ mol^{-1} (intercept approximately 1% of fitted ΔS) ($F_{1,90}$ = 1.23 · 10^5, R^2 = 0.9993, P < 2.2 · 10^{-16}) (Fig. 2f). Meanwhile V_{cmax25} was identical between both approaches with a slope of 1.000 ± 1.1 · 10^{-5} (intercept not significant; $F_{1,91}$ = 8.2 · 10^9, R^2 = 1.000, P < 2.2 · 10^{-16}) (Fig. 3b). For J_{max}, there were small differences in the fitting of E_a for J_{max}, with a slope of 0.998 ± 2 · 10^{-3} and intercept of -2.230 ± 1.08 · 10^{-1} kJ mol^{-1} ($F_{1,91}$ = 3.3 · 10^5, R^2 = 0.9997, P < 2.2 · 10^{-16}) (Fig. 2d). For ΔS, the slope was 0.962 ± 3 · 10^{-3} and an intercept of 0.025 ± 2 · 10^{-3} kJ mol^{-1} (intercept approximately 5% of fitted ΔS) ($F_{1,90}$ = 1.1 · 10^5, R^2 = 0.9992, P < 2.2 · 10^{-16}) (Fig. 2h). Meanwhile J_{max25} was identical between both approaches with a slope of 1.000 ± 1.2 · 10^{-5} (intercept not significant; $F_{1,92}$ = 6.7 · 10^9, R^2 = 1.000, P < 2.2 · 10^{-16}) (Fig. 3d).

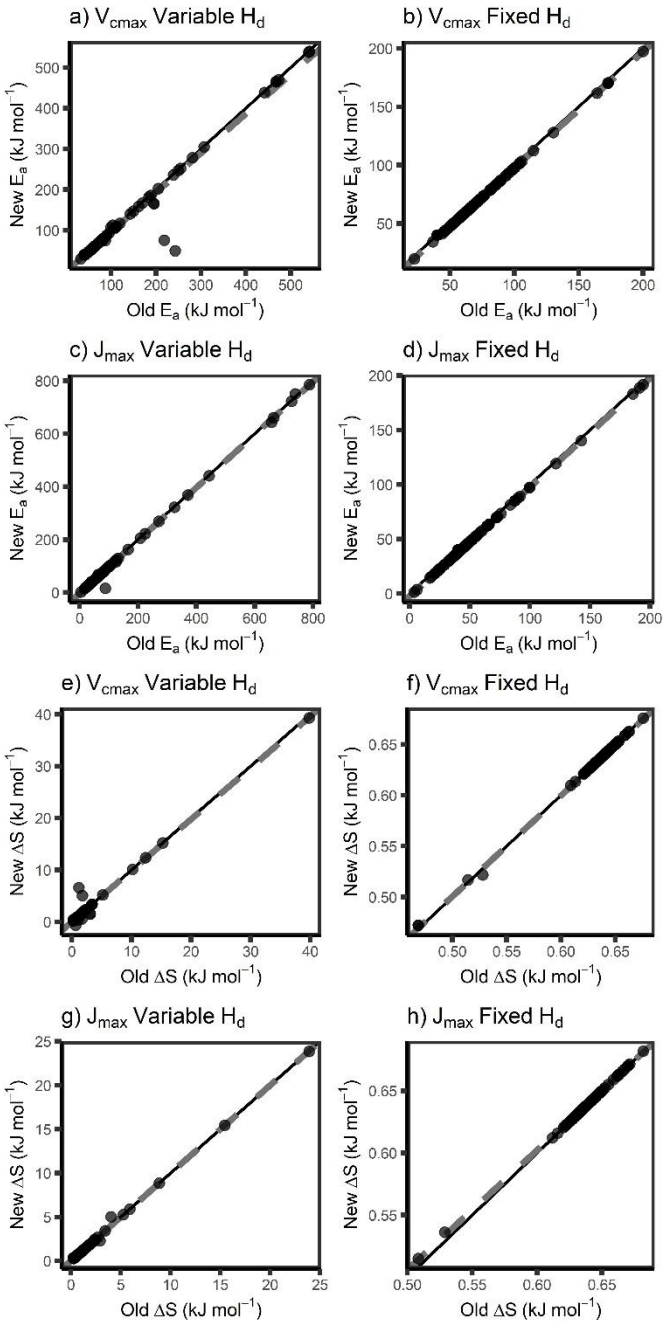

Figure 2 – The modified Arrhenius equation with the missing term (Equation 10) gives similar temperature response parameters as Equation 3 for E_a (a-d) and ΔS (e-h) for both V_{cmax} (a, b, e, f) and J_{max} (c, d, g, h) under scenarios where H_d is allowed to vary (a, c, e, g) and is fixed to 200 kJ mol^{-1} (b, d, f, h). "New" indicates Equation 10, "Old" indicates Equation 3. E_a: activation energy, ΔS: entropy parameter, H_d: deactivation energy, V_{cmax}: maximum capacity of rubisco carboxylation, J_{max}: maximum rate of electron transport. Black line indicates 1:1 line and grey dashed line indicates respective modeled slopes and intercepts.

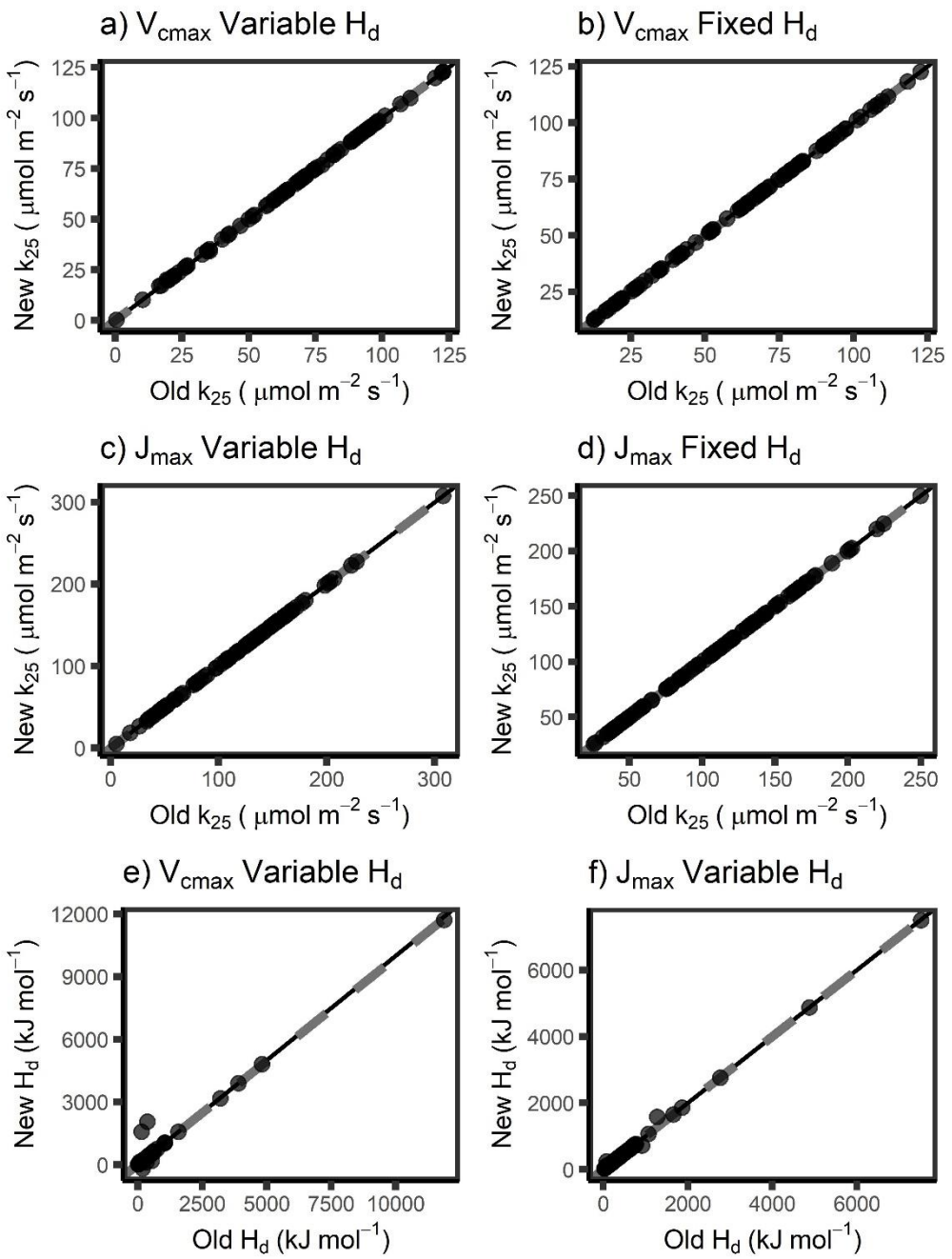

Figure 3 – The modified Arrhenius equation with the missing term (Equation 10) gives similar temperature response parameters as Equation 3 for k_{25} (a-d) and H_d (e, f) for both V_{cmax} (a, b, e) and J_{max} (c, d, f) under scenarios where H_d is allowed to vary (a, c, e, f) and is fixed to 200 kJ mol^{-1} (b, d). "New" indicates Equation 10, "Old" indicates Equation 3. k_{25}: rate of the process at 25 °C, H_d: deactivation energy, V_{cmax}: maximum capacity of rubisco carboxylation, J_{max}: maximum rate of electron transport. Black line indicates 1:1 line and grey dashed line indicates respective modeled slopes and intercepts.

Variable H_d

Incorporating the missing term into Equation 3 to produce Equation 10 caused small differences in the fitting of E_a for V_{cmax}, with a slope of 0.966 ± 2.6 · 10^{-2} (intercept not significant; $F_{1,74}$ = 3005, R^2 = 0.976, $P < 2.2 \cdot 10^{-16}$) (Fig. 2a). For ΔS, the slope was 0.989 ± 1.7 · 10^{-2} (intercept not significant; $F_{1,74}$ = 3339, R^2 = 0.9783, $P < 2.2 \cdot 10^{-16}$) (Fig. 2e), while H_d had a slope of 0.992 ± 1.9 · 10^{-2} (intercept not significant; $F_{1,74}$ = 2812, R^2 = 0.9744; $P < 2.2 \cdot 10^{-16}$) (Fig. 3e). Meanwhile V_{cmax25} was nearly identical between both approaches with a slope of 1.000 ± 4 · 10^{-3} (intercept not significant; $F_{1,74}$ = 7.98 · 10^6, R^2 = 1.000, $P < 2.2 \cdot 10^{-16}$) (Fig. 3a). For J_{max}, there were small differences in the fitting of E_a for J_{max}, with a slope of 1.000 ± 5 · 10^{-3} and an intercept of -3.119 ± 1.089 kJ mol^{-1} ($F_{1,80}$ = 3.6 · 10^4, R^2 = 0.9978, $P < 2.2 \cdot 10^{-16}$) (Fig. 2c). ΔS was identical, the slope was 1.000 ± 4 · 10^{-3} (intercept not significant; $F_{1,81}$ = 6.4 · 10^4, R^2 = 0.9987, $P < 2.2 \cdot 10^{-16}$) (Fig. 2g), while H_d was identical with a slope of 1.000 ± 4 · 10^{-3} (intercept not significant; $F_{1,81}$ = 5.2 · 10^4, R^2 = 0.9985; $P < 2.2 \cdot 10^{-16}$) (Fig. 3f). J_{max25} was identical between both approaches with a slope of 1.000 ± 1 · 10^{-3} (intercept not significant; $F_{1,81}$ = 5.8 · 10^7, R^2 = 1.000, $P < 2.2 \cdot 10^{-16}$) (Fig. 3c).

Impacts on modelled net carbon balance

In general, the differences in thermal response parameters were amplified when integrated at the whole-plant level. For daily photosynthesis (A) measured at a fixed H_d of 200 kJ mol^{-1}, the slope for the low respiration model was 0.977 ± 7.666 · 10^{-3} and an intercept of 0.002 ± 9.366 · 10^{-5} (approximately 2% of modeled A) ($F_{1,898}$ = 1.625 · 10^6, R^2 = 0.9994; $P < 2.2 \cdot 10^{-16}$) (Fig. 4b). Similarly, the high respiration model for A had a slope of 0.977 ± 7.666 · 10^{-3} and an intercept of 0.004 ± 1.591 · 10^{-3} (approximately 2% of modeled A) ($F_{1,898}$ = 1.625 · 10^6, R^2 = 0.9994; $P < 2.2 \cdot 10^{-16}$) (Fig. 4d). For daily A measured at a variable H_d, the slope for the low respiration model was 0.983 ± 9.909 · 10^{-3} and the intercept was 0.002 ± 1.128 · 10^{-3} (approximately 2% of modeled A) ($F_{1,556}$ = 9.834 · 10^5, R^2 = 0.9994; $P < 2.2 \cdot 10^{-16}$) (Fig. 4a). For the high respiration model of daily A, the slope was 0.983 ± 9.909 · 10^{-3} and the intercept was 0.003 ± 9.909 · 10^{-4} (approximately 2% of modeled A) ($F_{1,556}$ = 9.834 · 10^5, R^2 = 0.9994; $P < 2.2 \cdot 10^{-16}$) (Fig. 4c).

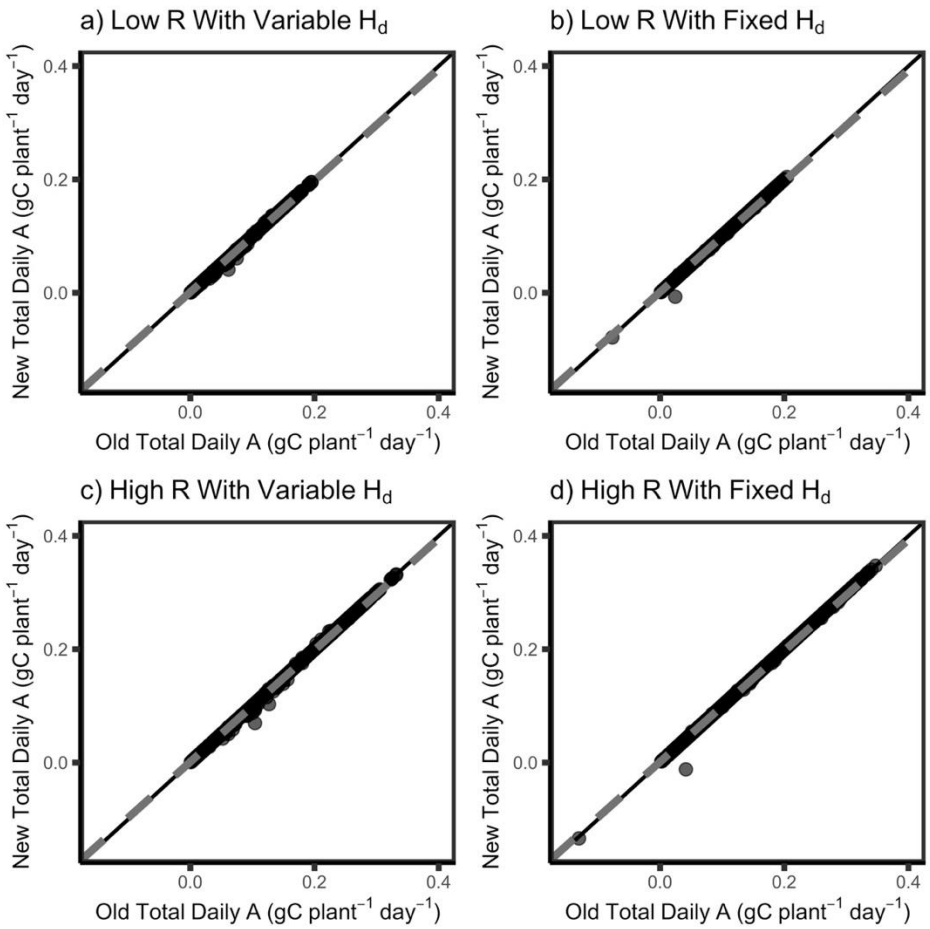

Figure 4 – The modified Arrhenius equation with the missing term (Equation 10) gives slight differences in modeled total daily photosynthesis compared to Equation 3 for low R (a,b) and high R (c,d) under scenarios where H_d is allowed to vary (a, c) and is fixed to 200 kJ mol^{-1} (b,d). "New" indicates Equation 10, "Old" indicates Equation 3. A: photosynthesis, Low R: low respiration, High R: high respiration. Black line indicates 1:1 line and grey dashed line indicates respective modeled slopes and intercepts.

The ratio of the total daily photosynthesis : respiration (A/R) was also considered when comparing models. Using a fixed H_d of 200 kJ mol^{-1}, the low respiration model of A/R had a slope of 0.993 ± 5.634 · 10^{-3} and the intercept was 0.025 ± 0.002 (approximately 1% of modeled A/R) ($F_{1,898}$ = 3.109 · 10^6, R^2 = 0.9997; P <2.2 · 10^{-16}) (Fig. 5b). The high respiration model of A/R was similar; the slope was 0.993 ± 5.628 and the intercept was 0.014 ± 0.001 (approximately 1% of modeled A/R) ($F_{1,898}$ = 3.115 · 10^6, R^2 = 0.9997; P <2.2 · 10^{-16}) (Fig. 5d). Using a variable H_d, the low respiration model of A/R had a slope of 0.994 ± 0.001 and the intercept was 0.030 ± 0.001 (approximately 1% of modeled A/R) ($F_{1,556}$ = 6.857 ·

10^5, R^2 = 0.9992; $P < 2.2 \cdot 10^{-16}$) (Fig. 5a). The high respiration model had a similar slope of 0.994 ± 0.001 and the intercept was 0.017 ± 0.003 (approximately 1% of modeled A/R) ($F_{1,556} = 6.812 \cdot 10^5$, R^2 = 0.9992; $P < 2.2 \cdot 10^{-16}$) (Fig. 5c).

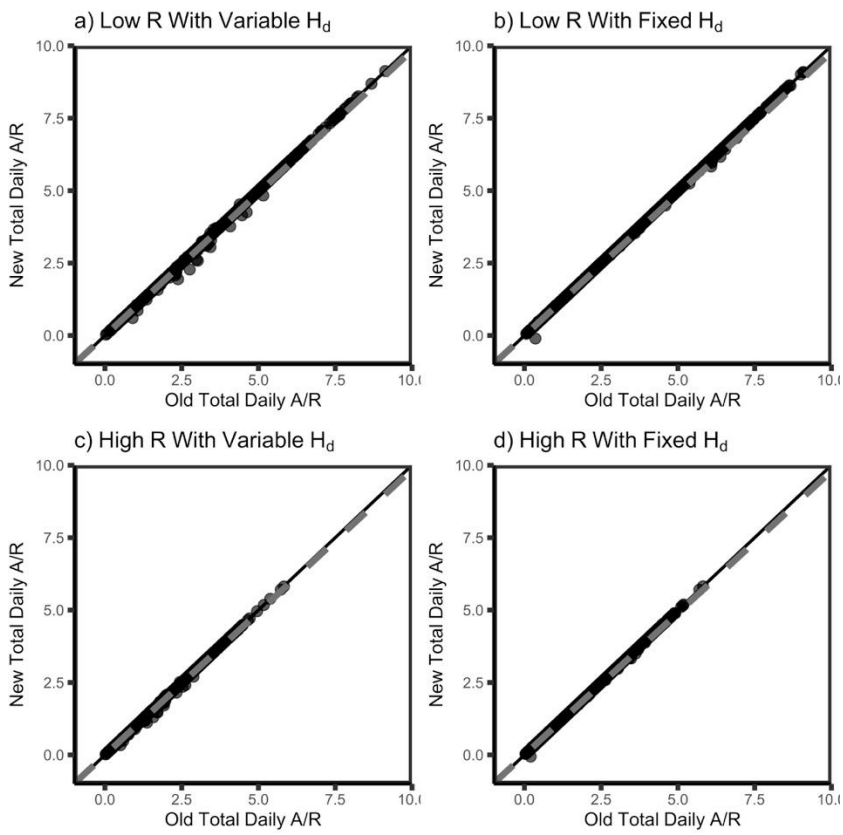

Figure 5 – The modified Arrhenius equation with the missing term (Equation 10) gives slight differences in modeled total daily A/R compared to Equation 3 for low R (a,b) and high R (c,d) under scenarios where H_d is allowed to vary (a, c) and is fixed to 200 kJ mol^{-1} (b,d). "New" indicates Equation 10, "Old" indicates Equation 3. A: photosynthesis, R: respiration, Low R: low respiration, High R: high respiration. Black line indicates 1:1 line and grey dashed line indicates respective modeled slopes and intercepts.

Lastly, total daily carbon (C) gain was also compared between models with different thermal response parameters. Using a fixed H_d of 200 kJ mol^{-1}, the low respiration model of total C gain had a slope of 0.978 ± $7.445 \cdot 10^{-4}$ and an intercept of 0.001 ± $7.609 \cdot 10^{-5}$ (approximately 2% of modeled C gain) ($F_{1,898} = 1.726 \cdot 10^6$, R^2 = 0.9995; $P < 2.2 \cdot 10^{-16}$) (Fig. 6b). Likewise, the high respiration of total C gain had a slope of 0.979 ± $7.261 \cdot 10^{-4}$ and an intercept of 0.001 ± $1.116 \cdot 10^{-4}$ (approximately 2% of

modeled C gain) ($F_{1,898}$ = 1.821 · 10^6, R^2 = 0.9995; P <2.2 · 10^{-16}) (Fig. 6d). This can be compared to a variable H_d; starting with the low respiration model, total C gain had a slope of 0.985 ± 9.555 · 10^{-4} and an intercept of 0.001 ± 1.223 · 10^{-3} (approximately 1.5% of modeled C gain) ($F_{1,556}$ = 1.06 · 10^6, R^2 = 0.9995; P <2.2 · 10^{-16}) (Fig. 6a). The high respiration of total C gain also had a slope of 0.985 ± 9.110 · 10^{-4} and an intercept of 0.001 ± 1.290 · 10^{-4} (approximately 1.5% of modeled C gain) ($F_{1,556}$ = 1.17 · 10^6, R^2 = 0.9995; P <2.2 · 10^{-16}) (Fig. 6c).

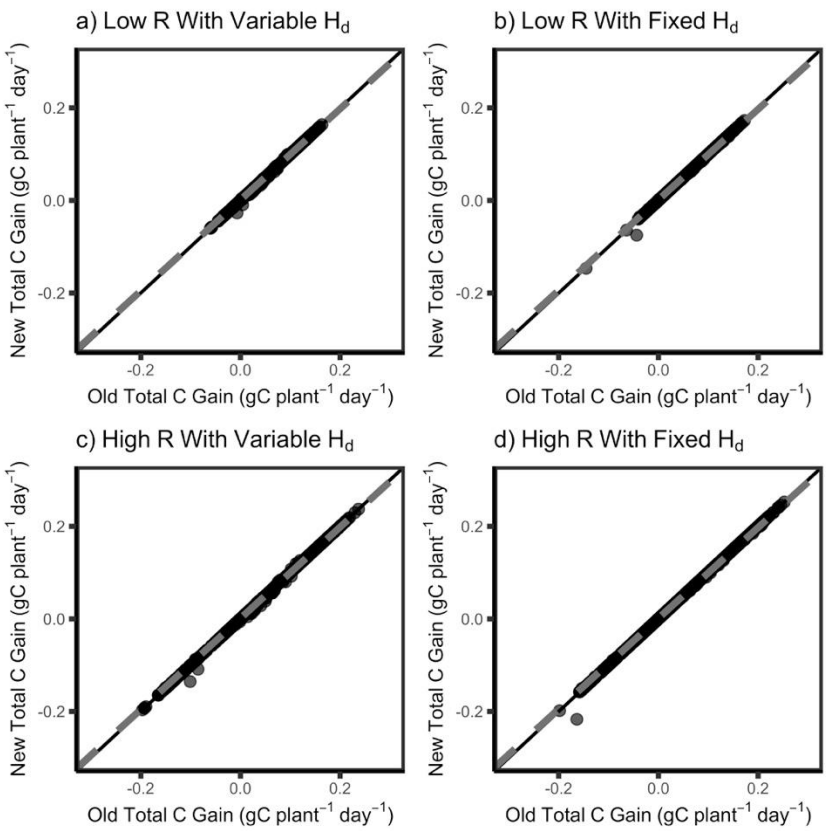

Figure 6 – The modified Arrhenius equation with the missing term (Equation 10) gives slight differences in modeled total carbon gain compared to Equation 3 for low R (a,b) and high R (c,d) under scenarios where H_d is allowed to vary (a, c) and is fixed to 200 kJ mol^{-1} (b,d). "New" indicates Equation 10, "Old" indicates Equation 3. C: carbon, Low R: low respiration, High R: high respiration. Black line indicates 1:1 line and grey dashed line indicates respective modeled slopes and intercepts.

Discussion

We sought to determine whether the missing term in Equation 3 had a meaningful impact on fitted temperature response parameters due to its prevalence in photosynthetic temperature response data and vegetation modeling (Kattge & Knorr, 2007; Duursma & Medlyn, 2012; Rogers et al., 2017; Smith & Dukes, 2017; Stinziano et al., 2018; Stinziano et al., 2019; Kumarathunge et al., 2019). Our present analysis suggests that there is no large impact on the fitted temperature response parameters for V_{cmax} and J_{max}, with differences ranging between 0 and 3.8% depending on the parameter. In general, fitting Equation 10 instead of Equation 3 results in slightly reduced values for E_a and ΔS, with essentially no impact for k_{25} and H_d when H_d is fit. When H_d is fixed, there are no meaningful differences in the fits except for ΔS for J_{max}, where Equation 10 values are ~4% lower than Equation 3 values, and intercepts in the E_a regressions of ~-2 kJ mol^{-1}, which represents <5% differences between the two equations in most instances. These findings are promising in that one of the parameters to which modelled carbon gain is particularly sensitive, H_d (Stinziano et al., 2018), is minimally affected by the missing term. However, since temperature responses are non-linear, small changes in the shape of an accelerating curve can have a strong impact on the integral of the response (Jensen, 1906). This caused the differences in temperature response parameters to cause ~1.5 – 2.2% difference in daily C balance. The daily C balance was most affected by the missing term in Equation 3 when comparing models where H_d was fixed, leading to a 2.2% change. Overall, comparisons of low-respiration to high-respiration scenarios resulted in similar percent changes in daily C balance; however, the variation was consistently larger under high-respiration across all variables measured. Similar trends were found when comparing differences in daily photosynthesis and A/R.

Based on the above analysis, the impact of the missing term in the modified Arrhenius equation may appear negligible based on the parameter outputs. However given that carbon balance is the time integral of net CO_2 assimilation, this may lead to substantial impacts over a long time period. It is thus possible that the apparently small differences we observed could accumulate to relatively large carbon flux errors across large spatial and temporal scales with fluctuating temperatures. A growing body of literature on using Optimality Theory for estimating V_{cmax25} and J_{max25} (Ali et al., 2016; Walker et al., 2017; Smith et al., 2019) still relies on Equation 3 for temperature scaling. Given the impacts we observed, Optimality Theory may be even more successful if the temperature scaling were done

either with Equation 10, or, as we recommend, macromolecular rate theory which is better grounded in thermodynamics (e.g. Hobbs et al., 2013; Liang et al., 2018).

Since Equation 3 is incorrect, there are three arguments to support moving beyond the modified Arrhenius paradigm: 1) there are new approaches to modeling biological temperature responses that are better-grounded in thermodynamics (e.g. Macromolecular Rate Theory; Hobbs et al., 2013; Liang et al., 2018); 2) uncertainties in model outputs may accumulate due to the missing term across large spatial and temporal scales, and 3) the modified Arrhenius model as implemented is categorically incorrect due to a missing term. Therefore, we conclude that future modeling efforts should move beyond this incorrect paradigm.

Acknowledgments

We would like to thank Wesley J. Noe at the University of New Mexico for providing climate data. This research was supported by personal funds.

References

Ali AA, Xu C, Rogers A, Fisher RA, Wullschleger SD, Massoud EC, Vrugt JA, Muss JD, et al. 2016. A global scale mechanistic model of photosynthetic capacity (LUNA V1.0). Geoscientific Model Development 9:587-606.

Amthor JS. 2000. Direct effect of elevated CO2 on nocturnal in situ leaf respiration in nine temperate deciduous tree species is small. Tree Physiology 20: 139–144.

Arrhenius S. 1915. Quantitative laws in biological chemistry. Bell: London.

Atkin OK, Tjoelker MG. 2003. Thermal acclimation and the dynamic response of plant respiration to temperature. Trends in Plant Science 8:343-351.

Ayub G, Smith RA, Tissue DT, Atkin OK. 2011. Impacts of drought on leaf respiration in darkness and light in *Eucalyptus saligna* exposed to industrial-age atmospheric CO_2 and growth temperature. New Phytologist 190: 1003-1018.

Bernacchi CJ, Singsaas EL, Pimentel C, Portis Jr AR, Long SP. 2001. Improved temperature response functions for models of rubisco-limited photosynthesis. Plant Cell and Environment 24:253-259.

Ciais P, Sabine C, Bala G, Bopp L, Brovkin V, Canadell J, Chhabra A, DeFries R, Galloway J, Heimann M. 2013. Carbon and Other Biogeochemical Cycles. In: Heinze C, Tans P, Vesala T, eds. Climate Change 2013: The Physical Science Basis. Cambridge, UK, and New York, NY, USA: Cambridge University Press.

Duursma RA, Medlyn BE. 2012. MAESPA: a model to study interaction between water limitation, environmental drivers and vegetation function at tree and stand levels, with an example application to [CO_2] x drought interactions. Geoscientific Model Development 5:919-940.

Elzhov TV, Mullen KM, Spiess A-N, Bolker B. 2016. minpack.lm: R Interface to the Levenberg-Marquardt nonlinear least-squares algorithm found in MINPACK, plus support for bounds. R package version 1.2-1. https://CRAN.R-project.org/package=minpack.lm

Farquhar GD, et al. 1980. A biochemical model of photosynthetic CO_2 assimilation in leaves of C_3 species. Planta 149: 78-90.

Harley PC, Sharkey TD. 1991. An improved model of C_3 photosynthesis at high CO2: reversed O2 sensitivity explained by lack of glycerate re-entry into the chloroplast. Photosynthesis Research 27:169-178.

Heskel MA, O'Sullivan OS, Reich PB, Tjoelker MG, Weerasinghe LK, Penillard A, Egerton JJG, et al. 2016. Convergence in the temperature response of leaf respiration across biomes and plant functional types. Proceedings of the National Academy of Sciences USA 113: 3832-3837.

Hobbs JK, Jiao W, Ester AD, Parker EJ, Schipper LA, Arcus VL. 2013. Change in heat capacity for enzyme catalysis determines temperature dependence of enzyme catalyzed rates. ACS Chemical Biology 8:2388-2392.

Jensen JLWV. 1906. Sur les fonctions convexes et les inégalités entre les valeurs moyennes. Acta Mathematica 30: 175-193.

Johnson FH, Eyring H, Williams RW. 1942. The nature of enzyme inhibitions in bacterial luminescence: sulfanilamide, urethane, temperature and pressure. Journal of Cellular and Comparative Physiology 20:247-268.

Kattge J, Knorr W. 2007. Temperature acclimation in a biochemical model of photosynthesis: a reanalysis of data from 36 species. Plant, Cell & Environment 30:1176-1190.

382 Kruse J, Hopmans P, Adams MA. 2008. Temperature responses are a window to the physiology of dark
383 respiration: differences between CO_2 release and O_2 reduction shed light on energy
384 conservation. Plant, Cell Environment 31: 901-914.
385 Kumarathunge DP, Medlyn BE, Drake JE, Tjoelker MG, Aspinwall MJ, Battaglia M, Cano FJ, Carter KR,
386 Molly AC, Lucas AC, et al. 2019. Acclimation and adaptation components of the temperature
387 dependence of plant photosynthesis at the global scale. New Phytologist 222:768-784.
388 Kumarathunge DP, Medlyn BE, Drake JE, Tjoelker MG, Aspinwall MJ, Battaglia M, Cano FJ, Carter KR,
389 Molly AC, Lucas AC, et al. 2018. ACi-TGlob_V1.0: a global dataset of photosynthetic CO_2
390 response curves of terrestrial plants. doi: 10.6084/m9.figshare.7283567.v1.
391 Liang LL, Arcus VL, Heskel MA, O'Sullivan OS, Weerasinghe LK, Creek D, Egerton JJG, et al. 2018.
392 Macromolecular rate theory (MMRT) provides a thermodynamics rationale to underpin the
393 convergent temperature response in plant leaf respiration. Global Change Biology 24:1538-
394 1547.
395 Medlyn BE, Duursma RA, Eamus D, Ellsworth DS, Prentice IC, Barton CVM, Crous KY, et al. 2011.
396 Reconciling the optimal and empirical approaches to modelling stomatal conductance. Global
397 Change Biology 17:2134-2144.
398 Medlyn BE, Dreyer E, Ellsworth D, Forstreuter M, Harley PC, Kirschbaum MUF, Le Roux X, et al. 2002.
399 Temperature responses of parameters of a biochemically based model of photosynthesis. II. A
400 review of experimental data. Plant, Cell & Environment 25:1167-1179.
401 Norman JM, Campbell GS. 1998. An introduction to environmental biophysics. New York NY: Springer.
402 R Core Team. 2019. R: A language and environment for statistical computing. R Foundation for
403 Statistical Computing, Vienna, Austria. URL https://www.R-project.org/.
404 Rogers A, Medlyn BE, Dukes JS, Bonan G, von Caemmerer S, Dietze MC, Kattge J, et al. 2017. A
405 roadmap for improving the representation of photosynthesis in Earth system models. New
406 Phytologist 213:22-42.
407 Sharkey TD. 1985. Photosynthesis in intact leaves of C_3 plants – physics, physiology and rate
408 limitations. Botanical Review 51:53-105.
409 Smith NG, Dukes JS. 2017. Short-term acclimation to warmer temperatures accelerates leaf carbon
410 exchange processes across plant types. Global Change Biology 23:4840-4853.

411 Smith NG, Keenan TF, Prentice IC, Wang H, Wright IJ, Niinemets Ü, Crous KY, Domingues TF, et al.
412 2019. Global photosynthetic capacity is optimized to the environment. Ecology Letters 22:506-
413 517.
414 Stinziano JR, Murphy BK. 2020. arrhenius.comparison: comparing versions of the modified Arrhenius
415 equation. R package version 1.0.0.
416 Stinziano JR, Way DA. 2017. Autumn photosynthetic decline and growth cessation in seedlings of
417 white spruce are decoupled under warming and photoperiod manipulations. Plant, Cell and
418 Environment 40:1296-1316.
419 Stinziano JR, Way DA, Bauerle WL. 2018. Improving models of photosynthetic thermal acclimation:
420 which parameters are most important and how many should be modified? Global Change
421 Biology 24:1580-1598.
422 Stinziano JR, Bauerle WL, Way DA. 2019. Modelled net carbon gain responses to climate change in
423 boreal trees: impacts of photosynthetic parameter selection and acclimation. Global Change
424 Biology 25:1445-1465.
425 Walker AP, Quaife T, van Bodegom PM, De Kauwe MG, Keenan TF, Joiner J, Lomas MR, MacBean, et
426 al. 2017. The impact of alternative trait-scaling hypotheses for the maximum photosynthetic
427 carboxylation rate (V_{cmax}) on global gross primary production. New Phytologist 215:1370-1386.
428 Way DA, Yamori W. 2014. Thermal acclimation of photosynthesis: on the importance of adjusting our
429 definitions and accounting for thermal acclimation of respiration. Photosynthesis Research
430 119:89-100.
431 Weger HG, Guy RD. 1991. Cytochrome and alternative pathway respiration in white spruce (*Picea*
432 *glauca*) roots. Effects of growth and measurement temperature. Physiologia Plantarum 83:675-
433 681.
434